IBRACON Structures and Materials Journal
Revista IBRACON de Estruturas e Materiais
ISSN 1983-4195 ismj.org

ORIGINAL ARTICLE

Numerical analysis of physical barriers to mitigate the gas tank explosion effects using computational fluid dynamics

Análise numérica de barreiras físicas para mitigar os efeitos da explosão de tanques de gás usando fluidodinâmica computacional

Tiago Rodrigues Coelho de Moura[a]
Murilo Limeira da Costa Neto[b]
Graciela Nora Doz[a]

[a]Universidade de Brasília – UnB, Departamento de Engenharia Civil e Ambiental, Brasília, DF, Brasil
[b]Instituto de Educação Superior de Brasília – IESB, Departamento de Engenharia Civil, Brasília, DF, Brasil

Received 17 February 2023
Revised 07 May 2023
Accepted 20 May 2023
Corrected 27 March 2024

Abstract: In many urban buildings, there is the presence of gas central storage, which contain pressurized tanks. One of the main risks in these places is an explosion, which may or may not is followed by fire. In general, the shock wave formed by this phenomenon is disastrous and can cause material damage and even fatalities. Recent research has contributed to understanding protective systems against this phenomenon; however, it is necessary to advance in developing protection devices for gas central storage. From this perspective, the implementation plan of these devices in order to mitigate the harmful effects of explosions are essential to raise the safety level in construction. Physical protection barriers are appropriate solutions for the protection of buildings, especially in places where it is impossible to bury gas reservoirs. In addition to the potential to reduce back pressure levels, protective walls, when properly designed, can also prevent the spread of debris from the explosion. Another kind of barrier that influences the propagation of the shock wave close to the ground is the ditches, whose function is related to the absorption and redirection of wave energy. Understanding the positioning, geometry, and overpressure attenuation potential of physical barriers are essential in developing safer and more reliable projects. This article aims to study protective barriers in buildings with pressurized gas tanks. The study was developed numerically using the Autodyn software. This program is a tool based on computational fluid dynamics (CFD). The protective capacity of the proposed types of protection regarding the mitigation of incident overpressures was evaluated qualitatively and quantitatively.

Keywords: explosion, gas tank, shock wave, overpressure, protective barriers.

Resumo: Em muitas edificações urbanas há a presença de centrais de gás, as quais contém tanques pressurizados. Nesses locais, um dos principais riscos existentes é a explosão, que pode ser seguida ou não de incêndio. Em geral, a onda de choque formada por este tipo de fenômeno é desastrosa e pode ocasionar diversos danos materiais e até mesmo fatalidades. Pesquisas recentes têm contribuído para o entendimento dos sistemas protetivos contra este fenômeno, entretanto, é necessário avançar no desenvolvimento de dispositivos de proteção quanto as centrais de gás. Nessa perspectiva, a implementação destes para mitigação dos efeitos danosos das explosões é imprescindível para elevar o patamar de segurança nas construções. As barreiras físicas de proteção são soluções apropriadas para proteção de edificações, principalmente em locais onde há a impossibilidade de enterrar os reservatórios de gás. Além do potencial em reduzir os níveis de sobrepressão na parte posterior, os muros de proteção, quando corretamente projetados, também são capazes de impedir a propagação dos detritos oriundos da explosão. Outro tipo de barreira que influencia na propagação da onda de choque próxima ao solo são as valetas, cuja função está relacionada à absorção e redirecionamento da energia da onda. A compreensão sobre o posicionamento, geometria e potencial de atenuação de sobrepressões das barreiras físicas é indispensável no desenvolvimento de projetos mais seguros e confiáveis. Este artigo objetiva o estudo de barreiras protetivas em edificações com tanques de gás pressurizados. O estudo foi desenvolvido numericamente por meio do software Autodyn. Este programa é uma ferramenta baseada na dinâmica dos fluidos computacional (CFD). Avaliou-se

Corresponding author: Tiago Rodrigues Coelho de Moura. E-mail: tiago.trcm@gmail.com
Financial support: None.
Conflict of interest: Nothing to declare.
Data Availability: The data that support the findings of this study are available from the corresponding author, TRCM, upon reasonable request.
This document has an erratum: https://doi.org/10.1590/S1983-41952024000300011

qualitativamente e quantitativamente a capacidade protetiva dos tipos de proteção propostos quanto à mitigação das sobrepressões incidentes.

Palavras-chave: explosão, tanque de gás, onda de choque, sobrepressão, barreiras de proteção.

How to cite: T. R. C. Moura, M. L. Costa Neto, and G. N. Doz, "Numerical analysis of physical barriers to mitigate the gas tank explosion effects using computational fluid dynamics", *Rev. IBRACON Estrut. Mater.*, vol. 17, no. 3, e17301, 2024, https://doi.org/10.1590/S1983-41952024000300001

1 INTRODUCTION

Gas consumed by residential buildings, commerce, and industry is generally provided by pressurized tanks. The main risk associated with these gas reservoirs is an explosion, which can result in material damage and fatalities. In this way, damage mitigation mechanisms and energy dissipation devices are indispensable to increasing buildings' security level and reducing the event's lethality. For example, the use of physical protection barriers is an adequate solution to protect buildings sensitive to the effects of explosions.

In this sense, understanding explosion effects are essential in studying gas tanks. Explosions are phenomena that result in a sudden release of large energy amount, the source can be an explosive, pressurized steam, or a nuclear transformation [1]. About this phenomenon, fundamental studies approaching from elementary concepts to more complex formulations were presented by Zel'dovich and Raizer [2], Baker et al. [3], Kinney and Graham [1], and Needham [4]. According to Lees [5], the shock wave can transport from 40% to 80% of the explosion energy.

The explosion can be usually classified as chemical, mechanical or nuclear. This study focuses on mechanical explosions, which can originate from pressurized vessel rupture.

Liquefied petroleum gas (LPG) tanks are characterized as pressurized vessels, as they are subjected to high internal pressure to keep the gas in a liquid state. These containers must be constructed securely enough that a mechanical explosion will not occur.

Gas tanks can rupture due to several causes, such as corrosion, manufacturing defects, exposure to an intense heat source, and others. According to Salzano et al. [6], when a gas reservoir is subjected to a heat source, the evaporation of the liquid leads to an increase in internal pressure; in addition, the reservoir metallic wall suffers degradation in the mechanical properties due to the increase in temperature, mainly in the portion in contact with the steam.

Regarding the stored energy prediction in a gas tank, some models are available in the literature, and the main ones were gathered and presented by Molkov and Kashkarov [7]. As for the experimental approach, we can mention the research conducted by Tschirschwitz et al. [8] in which the explosion of several domestic gas tanks was analyzed. This research was essential for a preliminary validation analysis of the simulations in this article.

Physical barriers are elements constructed from various materials (concrete, steel, rocks, sand, soil, and trees, for example) whose purpose is to contain and absorb the explosion energy to mitigate its harmful effects on the surroundings. In this context, several studies (experimental and numerical) were developed to verify the efficiency of these barriers. The experiments carried out by Beyer [9] and Wu et al. [10] with concrete walls and those carried out by Xiao et al. [11] and Chen et al. [12] with gabion walls showed that these devices are capable of significantly reducing the overpressures in the back part, as they are a physical barrier to the passage of the shock wave. In the numerical field, relevant studies were conducted by Zhou and Hao [13], Soukup et al. [14], Taha et al. [15], Skob et al. [16], Attia et al. [17] showing the efficiency of these physical barriers with different geometries and scenarios. The use of trees as obstacles has been investigated experimentally in some relevant studies. Gebbeken et al. [18] analyzed barriers formed by two types of plants (Cherry laurel and Thuja), where Thuja was able to reduce the overpressure peaks behind the barrier by more than 60%. In a controlled environment (shock tube), Gan et al. [19] investigated the Juniperus Spartan plant; they found up to 23% reduction in overpressure behind the barrier formed by this vegetation. Under the effect of shock wave loading, masonry walls were analyzed by Browning et al. [20] experimentally and numerically. A comparative analysis between concrete walls and fences composed of juxtaposed steel bars with small spacing between them was conducted by Jin et al. [21].

This research contributed to the alternative study for protecting structures against the explosion effects; however, each of them is limited to specific scenarios and with the use of high explosives. In the field of gas tank explosions, there is a need to expand studies about protective measures thematic, as they are essential to guide good practices in gas central storage.

Numerical tools are indispensable in explosions study, as they allow analysis in highly complex environments since experiments can be expensive and dangerous. Currently, several tools based on CFD (Computational Fluid Dynamics) are available to researchers and designers, for example, Autodyn, FLACS, LS-DYNA, and STOKES (Shock Towards Kinetic Explosion Simulator).

STOKES is a computational code that solves a set of fluid mechanics equations using a mesh based on PDR (Porosity Distributed Resistance), according to Quaresma et al. [22]. This kind of porous mesh can consider small-scale obstacle effects without requiring substantial refinement [22].

Autodyn is a software that solves problems involving explosions, impacts, materials integrity, and others, where the results can be inserted into other Ansys® Workbench systems. In addition, as highlighted by Tham [23], this computational program has a unique characteristic which is the possibility of modeling the different parts of a single problem with the appropriate numerical formulation, thus allowing the user to couple different numerical solution techniques in a single problem. With this, Autodyn was adopted in this research.

In view of the above, this paper presents a study that aims to analyze physical obstacles efficiency to mitigate the effects of accidental explosions of gas tanks intended to supply buildings. In the numerical analyses, different geometries and dispositions of the protective devices are considered.

2 EXPLOSION OVERVIEW

Understanding some explosion parameters is indispensable in the analysis involving this phenomenon. This chapter exposes a brief theoretical summary of the shock wave and its properties. In addition, a model for predicting the energy stored in gas tanks and the equivalent mass of a high explosive is presented.

2.1 Shock wave overpressure

When an explosion occurs in the open air, the gaseous products suddenly expand out of the initially occupied volume, thereby creating a shock wave [24]. Figure 1 exemplifies the typical behavior of this wave, where P_0 is the ambient pressure, and P_{S0} is the maximum value of the positive phase. In general, the shock wave positive phase duration is short compared to the negative phase; however, the pressure magnitude is higher.

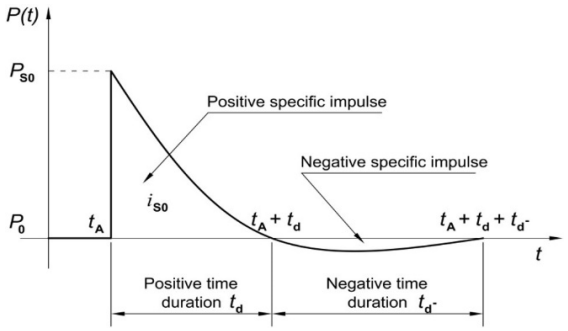

Figure 1. Typical blast wave pressure-time history [24].

The prediction of overpressure (difference between wave pressure and ambient pressure) in an environment with an explosion risk and it is mandatory in a preliminary damage assessment. In the literature, there are several equations to estimate the overpressure peaks. These equations are reliable because they are based on experiments; however, they do not capture the shock wave reflections properly. Equations 2 to 9 presented in Table 1 are some of the main models for the prognosis of overpressure in outdoor explosions, according to Costa Neto and Doz [25]. It is noteworthy that, for a gas tank explosion in the open air, Baker's model is widespread in the literature; however, it was not used in this work, as it also does not consider the effects of shock wave multiple reflections on obstacles.

Scaled distance (Equation 1) is necessary concept for the suitable application of the equations showed in Table 1. This parameter relates the distance from the explosive to the point of analysis with the mass of TNT in order to measure the effects of the explosion in terms of energy dispersion of the shock wave.

$$Z = \frac{r}{\sqrt[3]{W}} \tag{1}$$

Were Z = scaled distance (m/kg$^{1/3}$); r = distance from explosion center to analysis point (m); and W = TNT mass (kg).

Table 1. Overpressure prediction equations (ΔP) [25]

Author	Equation	Requirement	Unit
Brode	$\Delta P = \frac{6.7}{Z^3} + 1$ (2)	ΔP > 10	Bar
	$\Delta P = \frac{0.975}{Z} + \frac{1.455}{Z^2} + \frac{5.85}{Z^3} - 0,019$ (3)	0.1 < ΔP < 10	Bar
Henrych	$\Delta P = \frac{14.072}{Z} + \frac{5.540}{Z^2} - \frac{0.357}{Z^3} + \frac{0.00625}{Z^4}$ (4)	0.05 ≤ Z ≤ 0.3	Bar
	$\Delta P = \frac{6.194}{Z} - \frac{0.326}{Z^2} + \frac{2.132}{Z^3}$ (5)	0.3 ≤ Z ≤ 1	Bar
	$\Delta P = \frac{0.662}{Z} + \frac{4.05}{Z^2} + \frac{3.288}{Z^3}$ (6)	1 ≤ Z ≤ 10	Bar
Mill	$\Delta P = \frac{1772}{Z^3} - \frac{114}{Z^2} + \frac{108}{Z}$ (7)	-	kPa
Kinney	$\frac{\Delta P}{P_0} = \frac{808\left[1+\left(\frac{Z}{4.5}\right)^2\right]}{\sqrt{1+\left(\frac{Z}{0.048}\right)^2}\sqrt{1+\left(\frac{Z}{0.32}\right)^2}\sqrt{1+\left(\frac{Z}{1.35}\right)^2}}$ (8)	-	-
Newmark	$\Delta P = 6784\frac{W}{R^3} + 93\left(\frac{W}{R^3}\right)^{1/2}$ (9)	-	Bar

Shock wave interacts with obstacles when propagating through a medium, so the phenomena of reflection, refraction, and diffraction occur. In an open-air explosion, for example, the shock wave hits an obstacle, part of it is reflected and propagates through the air again in a different direction from incident one, and another part refracts, that is, it propagates through the obstacle itself. Shock wave reflection can cause a substantial increase in overpressure levels which, according to Cernak [26], is around two to nine times greater than the incident overpressure. Diffraction can be understood as the ability of the wave to circumvent objects; in the case of protection walls, Figure 2 exemplifies this phenomenon.

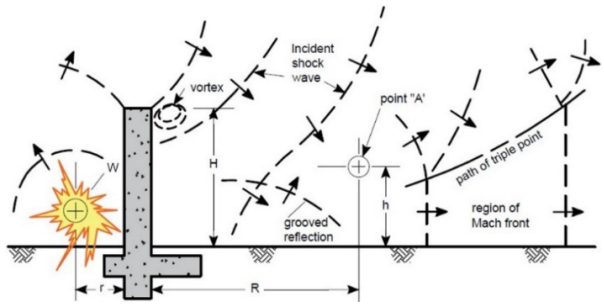

Figure 2. Shock wave diffraction over an obstacle [9].

2.2 TNT equivalent mass

In Autodyn, it is convenient to use a high explosive to simulate explosions, Trinitrotoluene (TNT) being one of the most appropriate for this purpose. Since most of the existing analytical formulations use TNT as a base, the gas tank's explosive capacity conversion to a TNT equivalent mass is necessary. According to Rodriguez and Schofield [27], the TNT equivalent mass as a function of the expansion energy of a given gas volume can be obtained by Equation 10.

$$W = \frac{E}{H_{TNT}} \tag{10}$$

Where W = TNT equivalent mass (kg); E = mechanical energy stored in the gas tank (J); and H_{TNT} = specific energy released in TNT detonation (J/kg). This specific energy is approximately equal to 4.184 MJ/kg, according to Bolonkin [28].

2.3 Energy prediction in pressurized tanks

Mechanical explosion is a high-intensity energy phenomenon resulting from vessel rupture with a high pressure differential between the inside and the outside. Adequate prediction of the energy involved in this process is necessary for studies involving gas tank explosions since, based on this information, a relationship can be established with a high explosive, in general, TNT. In the literature, several methods estimate the mechanical energy in a pressure vessel; in this sense, Molkov and Kashkarov [7] gathered some models for ideal and non-ideal gases. For LPG, these researchers suggest using the Abel-Noble state equation (Equation 11), as it represents a more realistic behavior of this gas and, consequently, improves the predictive capacity of the energy stored in the tank.

$$P\left(\frac{1}{\rho}-b\right)=RT \tag{11}$$

Where P = pressure (Pa); ρ = specific mass (kg/m^3); b = gas co-volume (m^3/kg); R = gas constant (J/kg·K); and T = temperature (K). Co-volume indicates the volume occupied by the gas molecules per unit mass.

In a hermetically sealed and pressurized tank, the mechanical energy is obtained by the product of the gas mass, temperature, and specific heat at constant volume [7]. Based on this assumption and introducing Equation 11, we have Equation 12, which allows us to predict the energy in a gas tank. The gas co-volume can be estimated using Equation 13, according to Çengel and Boles [29].

$$E=\left(\frac{P_g-P_0}{RT+b(P_g-P_0)}\right)V_g C_v T \tag{12}$$

$$b=\frac{RT_c}{8P_c} \tag{13}$$

Where E = stored mechanical energy (J); P_g = gas pressure inside the tank (Pa); P_0 = ambient pressure (Pa); V_g = pressurized gas volume (m^3); C_v = specific heat at constant volume (J/kg·K); T = gas temperature (K); b = gas co-volume (m^3/kg); R = gas constant (J/kg·K); T_c = temperature (K) at the critical point of the gas; and P_c = pressure (Pa) at the critical point of the gas. The ambient pressure is approximately equal to 101.325 kPa at sea level.

3 NUMERICAL SIMULATIONS

Numerical simulations were developed in Autodyn to analyze the efficiency of physical protection barriers against the gas tank explosion effects close to buildings. Preliminarily, two validation simulations were carried out; the first, based on experimental data, consisted of measuring the overpressures resulting from the explosion of domestic gas tanks. In the second, the validity of the two-dimensional model was verified. Subsequently, the physical protection barriers were analyzed in various positions and geometries; in addition, the influence of ditches on the ground was verified in terms of overpressures on the protective wall. An overview of the analysis environment is shown in Figure 3.

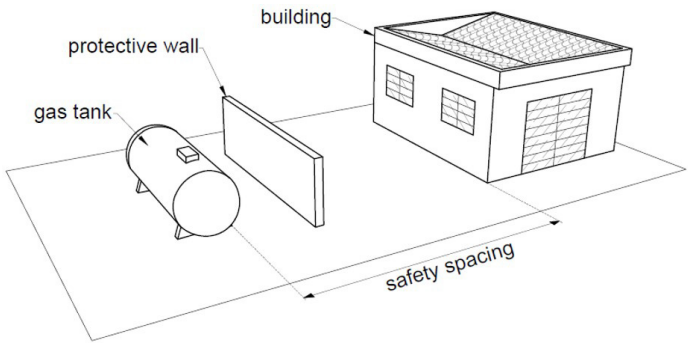

Figure 3. Analysis environment illustrative scheme.

3.1 Technical and regulatory parameters

Technical characteristics of tanks intended for gas storage are established by the manufacturer. This study adopted these characteristics from one of the largest European manufacturers. Reservoir volume limitation and distance from the building are criteria recommended by the Brazilian technical standard, ABNT NBR 13523 [30]. In order to meet the technical and regulatory requirements, the gas tank adopted in this part of the analysis has the parameters shown in Table 2. The technical standard mentioned above establishes that, for a distance of 7.5 m, the maximum volume must be equal to 8 m^3; however, among the volumes made available by the manufacturer, the chosen tank is the one closest to this normative limit, thus being appropriate for this study.

Table 2. Cylindrical gas tank characteristics.

Volume	**8.15 m^3**
Length	2580 mm
Diameter	2200 mm
Design pressure	2 MPa (20 bar)

3.2 Gas properties

LPG is a gas composed of several hydrocarbons, the main ones being propane and butane. In order to represent a more critical situation, the properties of propane were adopted (Table 3), as this gas requires greater pressure to liquefy compared to the other hydrocarbons in LPG.

Table 3. Propane gas properties [29].

Reference temperature (T)	**15º C (288.2 K)**
Specific heat at constant volume (C_v)	1.4909 kJ/kg·K
Gas constant (R)	0.1885 kJ/kg·K
Critical point temperature (T_c)	370 K
Critical point pressure (P_c)	4.26 MPa
Co-volume (b) – obtained by the Equation 13	0.00205 m^3/kg

3.3 Validation and energy loss

The main numerical validation process in this work was the same presented by Moura et al. [31]. These researchers compared the overpressure peaks from the domestic gas tank explosion obtained by numerical simulations with the results of the equations listed in Table 1 and with experimental data from Tschirschwitz et al. [8], as shown in Figure 4. These experiments analyzed the mechanical explosion of propane gas tanks subjected to a heat source.

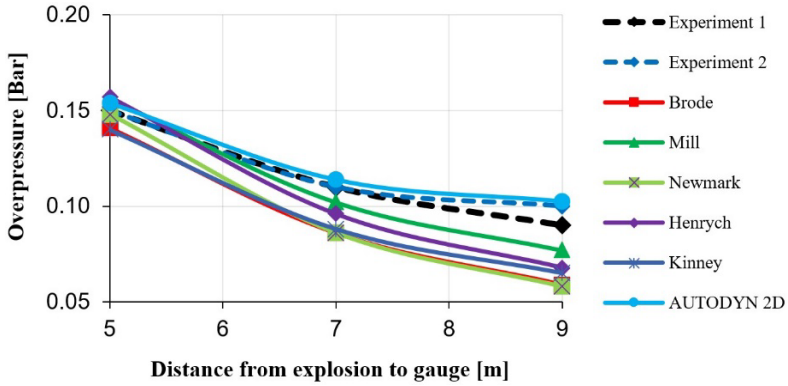

Figure 4. Overpressures from propane tanks explosion with a volume of 27.2 liters [31].

According to Borg et al. [32], in numerical models for consequence analysis, validation is viewed as an accuracy measure between model predictions and the real world. Furthermore, having a validated model implies confidence that the model is suitable for the intended purpose in terms of accuracy, uncertainty, and applicability. The results of validation model are shown in Figure 4, it was carried out in two-dimensional modelling, with axial symmetry and discretized with a 10 mm mesh. The air domain contains 4000 mm in height and 9200 mm in length. A strip of soil with a thickness of 100 mm was placed on the lower edge of the air to restrict the outflow; with this, the shock wave reflections could be analyzed. Gauges were inserted at 5, 7, and 9 m from the explosion center, the same positions as in the experiments from Tschirschwitz et al. [8]. Both the gauges and the explosion were placed 1200 mm from the ground. Boundary conditions for free air edges are "flow out" and "rigid" to the ground. Adopting the ground as a rigid surface was also a configuration used by Gebbeken et al. [18], who claim that the reflections obtained numerically are to some extent stronger than the real ones; however, the parameters needed to model the materials more realistically, especially soil, cannot be quantified with reasonable effort, so it is convenient to neglect them in simulations.

The energy released in an explosion is dissipated in various forms, for example, shock waves, sound, and debris. According to Lees [5], the shock wave carries about 40% to 80% of the explosion energy. In an overpressure analysis, the portion of energy not carried by the shock wave can be called energy loss. In the study presented by Moura et al. [31], this loss was estimated at approximately 25%. With this energy loss value, the TNT equivalent mass was estimated and modelled with spherical shape for a more uniform detonation energy distribution. Due the similarities of explosion events in the simulated models, these considerations were adopted in all simulations in this paper.

Based on the results of Figure 4, it is noted that the semi-empirical models diverged in the sensors 7 and 9 m from the explosion because they did not capture the effect of shock wave reflection; in this case, the numerical model was able to represent with reliable accuracy the phenomenon. The overpressures of the numerical model showed similar results with Tschirschwitz et al. [8] experiments, diverging by less than 4% in relation to experiment 2. These small differences can be related to the energy loss value considered, which was 25%, which is evidently appropriate for this problem.

3.4 Analysis model

3.4.1 Initial considerations

Figure 5 shows the model schematic layout used to evaluate the protective wall performance in reducing the overpressure peaks of the shock wave on the building facade. The model was discretized in full size in all simulations, and the dimensions of the air domain were adequate to cover the gas tank, wall, and building facade. Figure 6 shows the model discretization details in Autodyn interface, where the ground and the facade were considered rigid surfaces for the same reasons presented in item 3.3.

Physical barriers analyzed were concrete walls, gabion walls, and embankments. These protective devices were also considered rigid elements, and the adopted height is equal to 2300 mm in all simulations; this measure refers to the total height of the gas tank. All barriers were placed between the gas tank and the building and a distance D from the explosion point.

Luccioni et al. [33] cite that the precision of the numerical results is strongly dependent on the mesh size. However, the mesh size is limited by the model dimensions and the computer capacity. These researchers concluded that a 100 mm

mesh is sufficiently accurate for analyzing wave propagation in urban environments. To further improve the accuracy of the results, the simulations were performed with a 25 mm mesh in Autodyn 2D. In all simulations, the Euler processor was used for air and the Lagrange processor for solid materials.

The analysis procedure adopted in this article is a combined process involving analytical and numerical methods. The analytical methods are related to predicting the mechanical energy, the equivalent mass of TNT, and the overpressures in three points of the analysis environment. At these three points, there was no reflection effect before the direct incidence of the shock wave, and they served as an additional parameter for validating the simulations. All other analyzes (TNT detonation and shock wave propagation with multiple reflections) were performed using numerical methods using the Autodyn software.

The TNT equivalent mass was estimated based on the mechanical energy stored in the gas tank. For the proposed tank, this energy is equal to 114.185 MJ, which was calculated by Equation 12, whose variable values are shown in Tables 2 and 3. Since it is a problem similar to the preliminary validation analysis presented in item 3.3, the same energy loss was adopted (25%); consequently, when applying Equation 10, an equivalent mass of TNT equal to 20.468 kg was obtained. This explosive mass was considered spherical, initially discretized in a wedge (1D model), and later remapped in the 2D and 3D models.

In this work, chemical energy was neglected in the analysis since it only contributes to the formation of the shock wave by the gas cloud ignition.

Gauges 1, 2, and 3 were placed at points to record the pressure peaks along the facade, and gauges 4, 5, and 6 were placed in places where there was no reflection effect before the direct impact of the shock wave. The data captured by these last three sensors are compared with the results of applying the equations in Table 1 as an additional way of validating the simulations.

In addition to the physical protective barriers, additional analyses were proposed to alleviate the pressure on the protection wall face. These analyzes consisted of checking ditches placed in the ground between the wall and the gas tank. Details of the ditches are presented below in item 3.4.6.

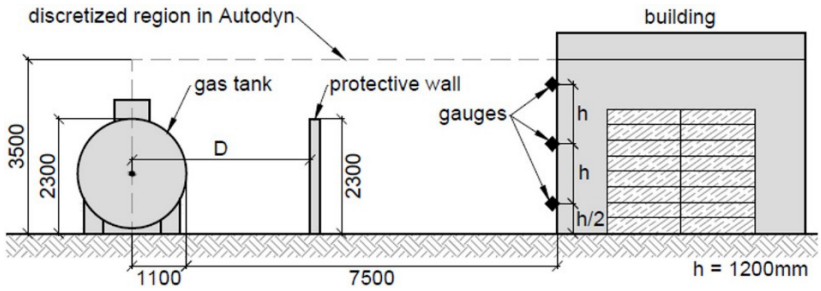

Figure 5. 2D analysis environment.

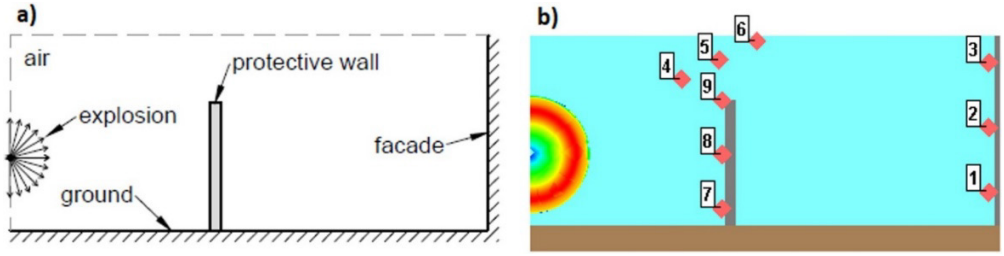

Figure 6. a) analysis model. b) model discretized in Autodyn.

3.4.2 2D model validity

2D analyses present a reliable cost-efficient approach for some problems, and its use may lead to a computational cost reduction. However, one must ensure that the results of this type of modeling do not depend fully on quantities or effects related to the third spatial dimension. In the case of protective walls with reduced length, the shock wave that goes around the sides can increase the overpressure levels at some points behind the wall due to multiple reflections.

This phenomenon was observed by Xiao et al. [11], who performed a convergence analysis varying the length (L) of the wall from 1 to 10 m and concluded that, for the scenario verified by them, the pressure peaks are not influenced when the length of the protective wall is equal to or greater than 7 m.

In order to evaluate the two-dimensional numerical modeling validity, some preliminary simulations were performed using a 3D model with a 100 mm mesh. In these simulations, the length of the wall was also checked with dimensions ranging from 1 to 10 m. The air domain dimensions were the following: the x-axis and y-axis have the same dimensions as the 2D model shown in Figure 5, and the z-axis has a dimension equal to 12000 mm. This z-axis measurement was adopted to cover the entire length of the 10 m long wall so that there was space for the shock wave to propagate along the sides.

3.4.3 Protective wall distance from explosion

Considering the standoff distances, the performance evaluation of the protective wall was made in three different positions, which were called P1, P2, and P3. The spacing distances are presented in Table 4, which indicates D in Figure 5. These spacing values were adopted in order to have good space for free circulation between the wall and the tank and also between the wall and the building.

Table 4. Protective wall distance from explosion

Wall position	D [mm]
P1	3600
P2	4850
P3	6100

3.4.4 Cross section geometry of physical protection barriers

The protection barriers cross section was analyzed with different geometries, as detailed in Figure 7 and Table 5. This table also presents the identification of each geometry. In addition to concrete walls, two other barrier types were verified, one representing a gabion wall and the other representing an embankment made with soil.

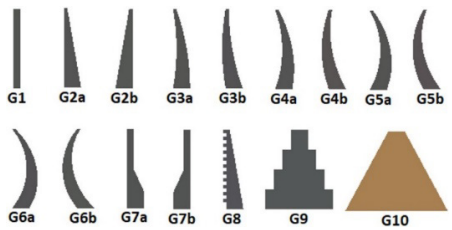

Figure 7. Cross section geometry of physical protection barriers.

Table 5. Physical barriers cross sections detailing

Model	Surface[1]	Curvature[2]	Width [mm]		Material
			Top	Base	
G1	plane	-	200	200	concrete
G2a	plane	-	100	500	concrete
G2b	inclined	-	100	500	concrete
G3a	concave	20°	100	500	concrete
G3b	convex	20°	100	500	concrete
G4a	concave	40°	100	500	concrete
G4b	convex	40°	100	500	concrete
G5a	concave	60°	100	500	concrete
G5b	convex	60°	100	500	concrete

Table 5. Continued...

Model	Surface[1]	Curvature[2]	Width [mm]		Material
			Top	Base	
G6a	concave	80°	100	500	concrete
G6b	convex	80°	100	500	concrete
G7a	plane	-	200	500	concrete
G7b	irregular	-	200	500	concrete
G8	rough	-	100	500	concrete
G9	steps	-	500	2000	concrete
G10	inclined	-	500	3000	sand

[1] *Kind of surface in the explosion front.* [2] *Curvature of the surface in the explosion front.*

In the wall of rectangular section, a thickness of 200 mm was adopted; this same measure was used by Song et al. [34] in the stress state investigation in protective concrete walls against explosions of tanks in gas central storage.

In general, concrete wall integrity is severely affected at their base close to the ground, which justifies the use of geometries with thicker bases. In the numerical study by Moura et al. [35], this fact was evidenced, and the use of a wall with a trapezoidal section (with a thickness of 100 mm at the top and 500 mm at the base) proved to be more resistant. In this work, the trapezoidal walls also have these measures mentioned above. In the G8 model, a roughness has been added on the blast wall front face. This roughness was formed by small squares with sides equal to 100 mm and spaced in the same measure.

Geometries with curved surfaces (concave and convex) were investigated with angles of 20º, 40º, 60º, and 80º, where the thickness was kept the same as the trapezoidal section. Analyzes similar to this one were also conducted by Taha et al. [15] and Attia et al. [17]; these researchers concluded that, in the scenario studied by them, a concave surface with a 60º curvature had a better performance in reducing overpressures in the region behind the wall.

The G7 model is a combination of the G1 wall and additional reinforcement in the region with the highest stress concentration. Thus, the total thickness of the base is equal to 500 mm. The vertical face of this reinforcement is equal to 500 mm, and the inclined surface has an angle of 25º with the vertical axis.

The G9 geometry represents a gabion barrier with base thickness of 2000 mm, a top of 500 mm, and steps height equal to 575 mm. These measures are appropriate for the construction of this type of apparatus. About gabion walls, Xiao et al. [11] state that the influence of porosity on the explosion energy distribution is difficult to specify. Therefore, for a primary interest regarding the propagation of the shock wave, it is appropriate to apply rigid boundary conditions and consider the surfaces flat. The material adopted for the G9 model was 35 MPa concrete because it has characteristics similar to rocks in terms of shock wave reflection.

The G10 model was created to represent an embankment, where the base has a width equal to 3000 mm and the top equal to 500 mm. The material adopted was sand because, in the Autodyn library, this material is the only one that can more appropriately represent the soil.

3.4.5 Protective wall's upper edge

Under the same objective (mitigating the explosion effects in the building), the protective wall's upper edge was also investigated. In this item, the rectangular cross-section (G1) was analyzed; however, the top edge was modified for specific configurations called B1, B2, B3, B4, and B5, as shown in Figure 8.

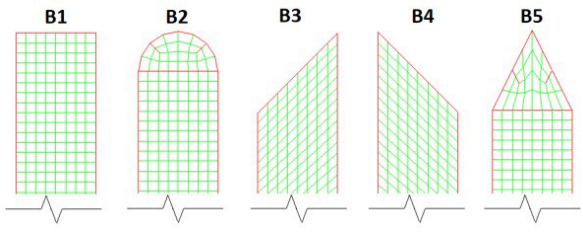

Figure 8. Protective wall top edges.

3.4.6 Ditch analysis for pressure relief on the protective wall

In order to relieve pressure on the protective wall front face and, consequently, reduce stress inside, ditches were installed in the ground between the wall and the explosion. Initially, a ditch 1 m deep and 0.5 m wide was adopted, forming a cross-sectional area equal to 0.5 m^2. This 0.5 m^2 area was used in all other models, as shown in Figures 9 and 10 and detailed in Table 6. The spacing distance between the wall and the ditch is 750 mm. This measure is sufficient for installing a proper foundation for the wall. In addition to the ditches, rough soil formed by small blocks with equal sides of 100 mm (Figure 10) was also verified. In these simulations, gauges 7, 8, and 9 were placed on the protective wall face with heights equal to 300, 1300, and 2300 mm, respectively.

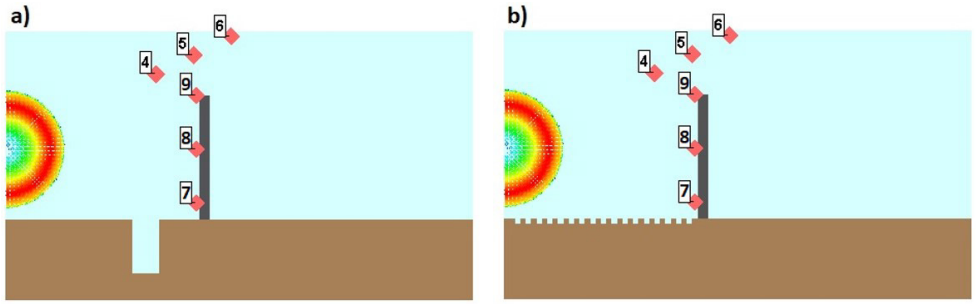

Figure 9. Discretization in Autodyn. a) ditch V1. b) rough soil.

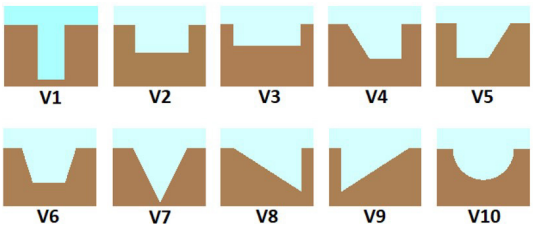

Figure 10. Ditches cross section geometry.

Table 6. Ditches cross section detailing.

Ditch	Depth [mm]	Width [mm]		Shape
		higher	bottom	
V1	1000	500	500	rectangular
V2	500	1000	1000	rectangular
V3	400	1250	1250	rectangular
V4	625	1000	600	trapezoidal
V5	625	1000	600	trapezoidal
V6	625	1000	600	trapezoidal
V7	1000	1000	0	triangular
V8	800	1250	0	triangular
V9	800	1250	0	triangular
V10	562.5	1125	0	semicircle

4 RESULTS AND DISCUSSIONS

This section presents the results and discussions about various simulations performed with the physical barriers to mitigate the effects of accidental gas tank explosions. The analysis consisted of verifying the position and geometry efficiency of the protective walls and some ditches for pressure relief in the protective wall itself. A validation check of the two-dimensional model due to the wall length was also carried out.

First, a numerical model check was performed to ensure the reliability of the simulations. In this step, the overpressures obtained in gauges 4, 5, and 6 of the 2D and 3D models were compared with the results calculated by the equations in Table 1. This verification of results between the numerical and analytical models was possible because, in these three sensors, the shock wave direct incidence occurred before any reflection effect. Figure 11 presents the results of these sensors, where this proximity and convergence were verified, mainly as one moves away from the explosion point. This procedure was an additional parameter in the validation of numerical models. The small differences between the 2D and 3D numerical models are mainly related to the mesh elements' size; however, they are close to each other. Gauges 4, 5, and 6 are 3.1305 m, 3.9131 m, and 4.6957 m away from the explosion center point, respectively.

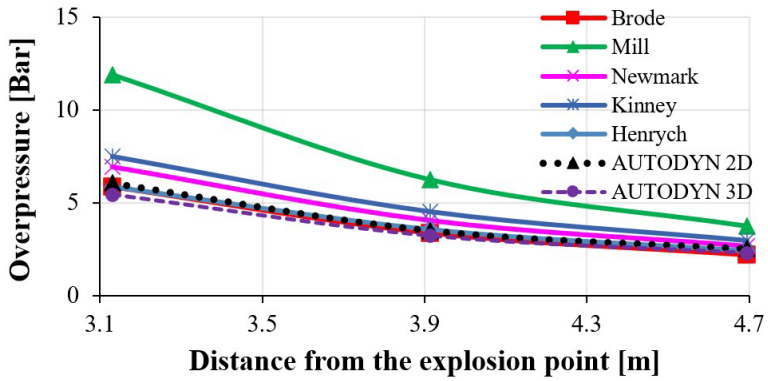

Figure 11. Overpressure in sensors 4, 5, and 6.

After the validation process described in the previous paragraph, the two-dimensional models' validity was also checked; the validation results are shown in Figure 12. It is noted that the protective wall length (L) directly influences the overpressure peaks on the building facade. Based on these results, it was verified that there is a convergence for length from 7 m, the same value found by Xiao et al. [11]. These researchers mentioned that this convergence depends on several factors, for example, the protective wall dimensions, the distance between the explosive and the protective wall, and also the distance between the protective wall and the construction. That said, it can be stated that, for the modeled scenario, the 2D numerical simulations are only valid if the wall length is equal to or greater than 7 m. In some cases (gauge 1 and L equal to 4 m, for example), the results showed that amplification in overpressure levels might occur. This phenomenon results from the multiple reflections of the wave fronts that go around the sides and above the protective wall and meet simultaneously on the building facade.

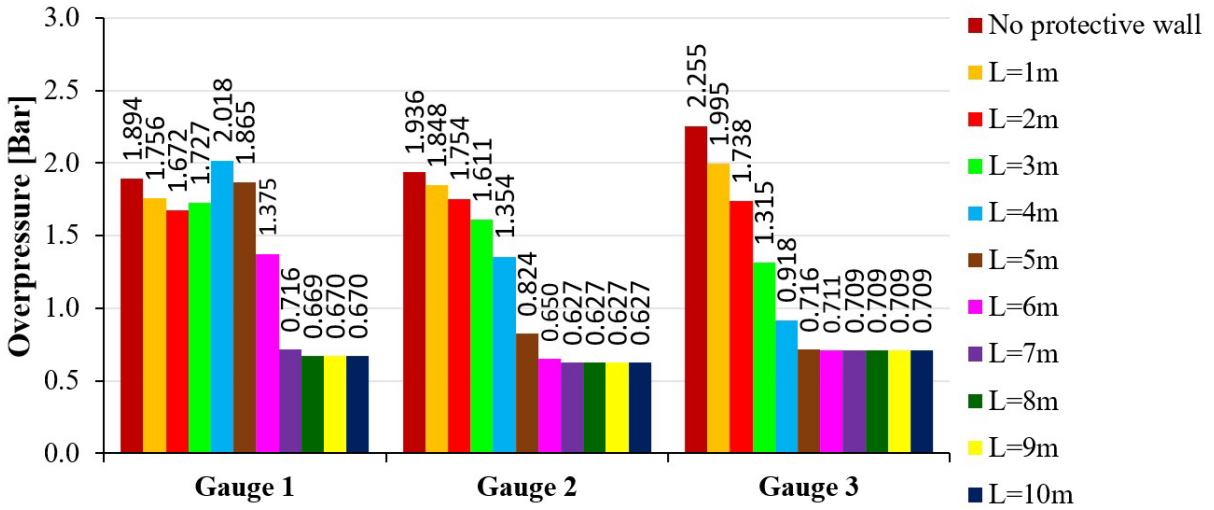

Figure 12. Overpressures on the building facade depending on the protective wall length.

The protective wall with G1 geometry was analyzed in three different positions, as detailed in Table 4. The overpressure peaks in gauges 1, 2, and 3 along the facade are shown in Figure 13. These results show that the analyzed protective wall was able to substantially reduce the shock wave effects on the building in all positions. However, among the verified positions, it was evident that the P1 position (wall closest to the gas tank) presents the best efficiency. Respectively for gauges 1, 2, and 3, the wall in position P1 reduced the overpressure peaks by 71.5%, 67.6%, and 72.1% concerning the no protective wall scenario. In gauges 1 and 2, there was some similarity in the wall efficiency for the three analyzed situations; however, in gauge 3 (the highest point of the facade), there were significant differences, resulting in position P3 being less efficient.

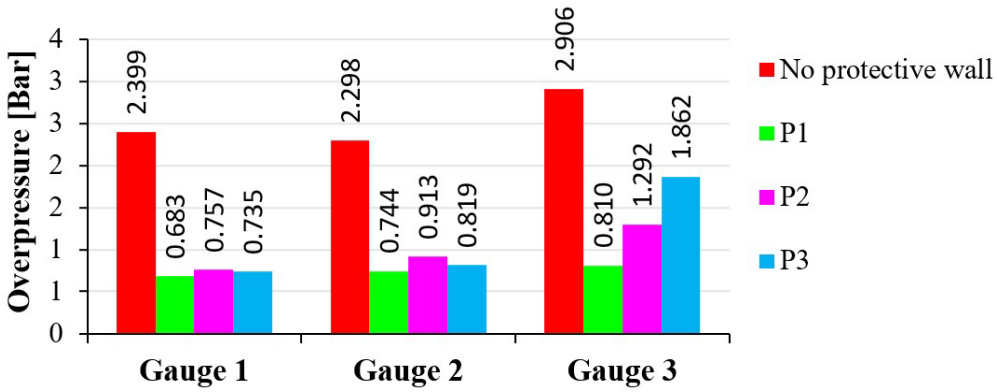

Figure 13. Overpressure on the building facade (gauges 1, 2, and 3) depending on the protective wall position.

The starting point for evaluating the geometries shown in Figure 7 was the protective wall simulation in position P1, as this position proved to be more efficient. Explored geometries are similar to real geometries in engineering designs. The analyses were performed under the efficiency criterion in attenuating the pressures on the building facade where gauges 1, 2, and 3 were positioned. The results obtained through numerical simulations are shown in Figure 14. Based on these results, it is noted that all geometries can perform their role in the model to a very satisfactory degree. In general, the verified barriers reduced the overpressure peaks between 59.4% and 74.4% concerning the unprotected model, as shown in Table 7. The results show no large variations in efficiency depending on the geometry; however, the G7a wall presented a better performance.

In general, when analyzing the curved geometries, it is noted that the concave models are more efficient than the convex ones, with the G6a (80º curvature) having the best performance. This fact can be observed in gauges 2 and 3 allocated on the building facade; in these cases, only in gauge 1 (closer to the ground), there was a better performance in some convex models. According to Taha et al. [15], when the incident wave hits a convex protective wall, it moves away from the wall in the upper and lower direction. As a result, the wave front directed upwards more easily circumvents the upper part of the protective wall and, consequently, raises the pressure levels at some measurement points. This shock wave behavior may also have occurred in the G10 model (landfill with inclined faces), which explains the high levels of overpressure when compared to the other models.

However, for the scenario simulated in this paper, geometries with curvatures similar to those studied by Taha et al. [15] and Attia et al. [17] did not prove advantageous when compared with simpler geometries, for example, G1, G2a, and G7a.

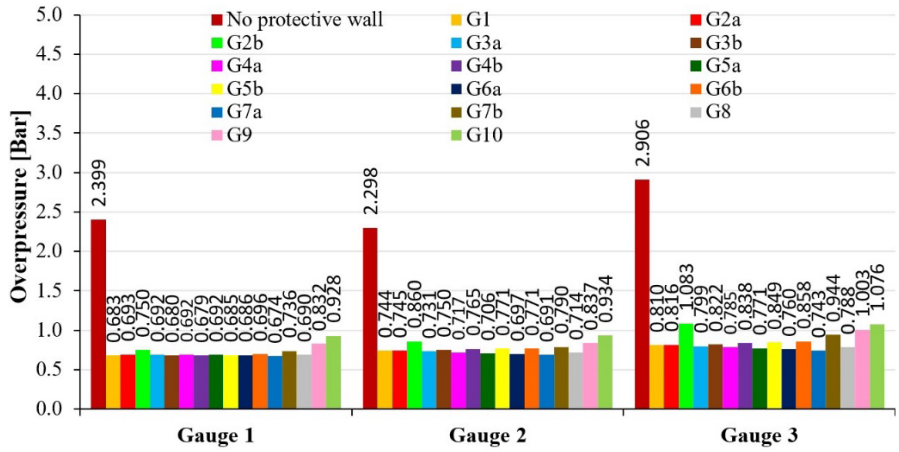

Figure 14. Overpressure on the building facade (gauges 1, 2, and 3) depending on the protective wall geometry.

Table 7. Percentage of overpressure peaks reduction for each type of barrier compared to the model without protective wall.

Gauge	G1	G2a	G2b	G3a	G3b	G4a	G4b	G5a
1	71.5%	71.1%	68.7%	71.2%	71.7%	71.1%	71.7%	71.2%
2	67.6%	67.6%	62.6%	68.2%	67.4%	68.8%	66.7%	69.3%
3	72.1%	71.9%	62.7%	72.5%	71.7%	73.0%	71.2%	73.5%
Gauge	**G5b**	**G6a**	**G6b**	**G7a**	**G7b**	**G8**	**G9**	**G10**
1	71.5%	71.4%	71.0%	71.9%	69.3%	71.2%	65.3%	61.3%
2	66.5%	69.7%	66.5%	69.9%	65.6%	68.9%	63.6%	59.4%
3	70.8%	73.9%	70.5%	74.4%	67.5%	72.9%	65.5%	63.0%

Regarding the top edge of the G1 wall, the results (Figure 15) showed a small variation between the values of overpressure peaks. For gauge point 1, edges B1 and B5 had equal results and were the most efficient. On gauge 2, edge B4 had the best performance, and on gauge 3, edge B1 was again more efficient.

In model B1, wave diffraction occurs with greater difficulty in relation to the others; in addition, the vortex generation on the upper edge of the protective wall (as exemplified in Figure 2) dissipates part of the wave front energy, consequently reducing the pressure on the building facade gauge. In the case of the semicircular model B2, the beginning of Mach reflection at the edge contour may occur; this phenomenon is presented by Needham [4], who compiled some studies on shock wave reflection on curved surfaces. For triangular edges, the wave slides more easily on the inclined edge, facilitating the diffraction phenomenon.

In general, it is noticed that more simplified geometries presented results as good or even superior to those of more complex geometries.

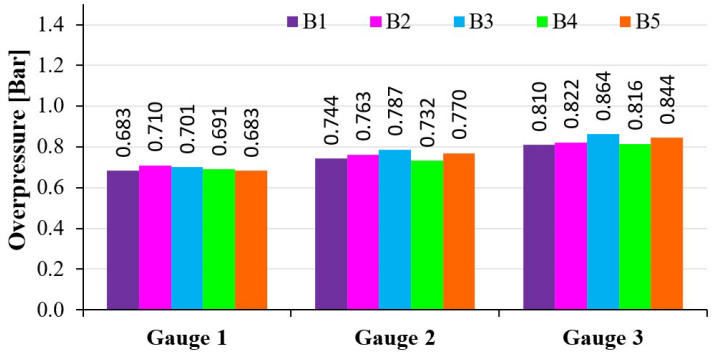

Figure 15. Overpressure on the building facade (gauges 1, 2, and 3) depending on the protective wall top edge.

After verifying the position and geometry, it is noted that the use of simpler geometries is adequate; however, in the case of the G1 wall (rectangular section), pressures can cause deterioration in the base due to the reduced thickness. In order to preserve the protective wall integrity, several types of ditches were analyzed, and the results are shown in Figure 16. These analyses adopted the concrete wall with geometry G1 in position P1. In addition, gauges 7, 8, and 9 were placed on the front face of the wall facing the explosion.

Based on the results (Figure 16), it is possible to observe that ditches and rough soil change the pressure levels mainly in the regions closest to the ground. These physical barriers were able to significantly reduce the overpressure peaks in gauges 7 and 8, while in gauge 9 there was no influence. In gauge 7, each ditch's geometry had a different efficiency, while in gauge 8, there was an approximation between the results.

The ditches exert influence on the shock wave propagation close to the ground, and this was observed by Soukup et al. [14], who mentions that the wave front bends and leaks into the ditch. This wave leakage into the ditch relieves the pressures and prevents the formation of the Mach reflection, which tends to originate at the ground surface when the shock wave reflected from the ground reaches incident one.

In the rough soil case, Lechat et al. [36] observed that roughness induces a delay in the formation of the Mach stem and also causes a decrease in the amplitude of the reflected shock. These phenomena explain the reduction of pressures due to the analyzed roughness.

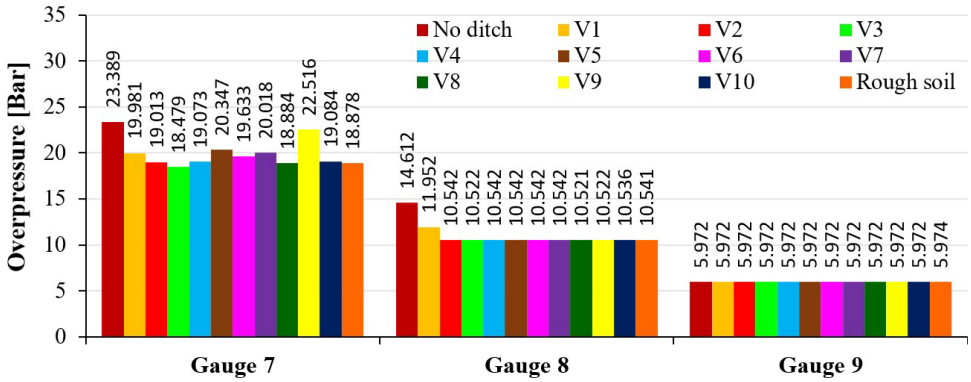

Figure 16. Overpressure on the protective wall front face (gauges 7, 8 and 9) for each type of ditch.

It was observed that the ditch depth could affect the protection mechanism's efficiency in relieving the shock wave overpressures. Figure 17 shows the results measured for ditch V3, where its depth (h) was varied, and overpressure peaks were reduced by up to 28%. For “h” equal to 100 mm, no positive or relevant effect was found that would justify its use. However, for ditches with greater depths, significant gains were obtained regarding the overpressures reduction. Furthermore, the results showed that the values converge as the depth increases. Thus, it is noted that excessively large depths are not necessary to obtain the mitigating effect of the shock wave.

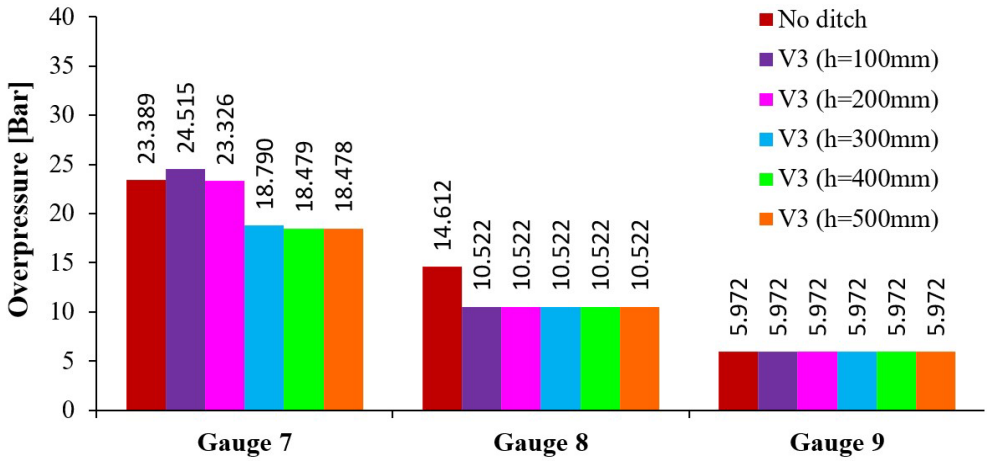

Figure 17. Overpressure on the protective wall front face (gauges 7, 8 and 9) for ditch V3 with different depths.

5 CONCLUSIONS

The analyzes carried out throughout this work sought to verify the protective barrier efficiency against the shock wave effects from the gas tanks bursting. The proposed models were elaborated and analyzed using Autodyn, which is a numerical tool based on CFD. As a complement to the numerical model, the TNT equivalent mass was obtained using an analytical equation. This approach, which combines analytical and numerical methods, proved to be appropriate for mechanical explosion studies of pressurized gas tanks.

Previously, an analysis of 2D model validation was carried out. The results showed that the physical barrier length influences the pressure peaks that affect the building. The 2D simulations are valid for the proposed scenario if the barrier length is equal to or greater than 7 m.

The protective barrier positioning concerning the gas tank and the building directly influences the pressure incident on the facade. The protective wall closer to the explosion point was observed to be more efficient. This may be related to the direct incidence region reduction of the shock wave on the facade and also due to the impediment of the Mach stem formation close to the ground.

Regarding the protective wall cross-section geometry, the results showed that the proposed geometries had similar results to each other, with only small variations occurring in the overpressure peaks at the measurement points. The most efficient geometry was the G7a (rectangular section wall with reinforcement in the posterior base), which is quite simple to build and has a reinforced base. Barriers with curved faces were as efficient as non-curved ones, so their use is not indicated due to the execution complexity. Regarding the upper edge of the wall, it was observed that there is some influence on the pressures; however, they were not so significant. In general, it became clear that the simplest geometries (walls with flat faces facing the explosion point, for example) are appropriate for the protective purpose of buildings with nearby gas tanks.

The ditch used to relieve pressure on the protective wall proved to be adequate, mainly for the region closest to the ground. The results showed that the rectangular ditch with a larger opening performed better for the designed purpose. In addition, it was verified that there is an ideal depth for pressure relief at the measurement points.

It is possible to note that duly validated numerical simulations are essential for understanding the protective barrier issue in scenarios with a pressurized tank explosion risk. The results presented in this work can be a useful contribution to assist the safety design of gas central storages, mainly in urban environments. Finally, it can be stated that the protective barrier use is a good measure in order to protect buildings and relevant places when there is no possibility of burying the gas tank.

REFERENCES

[1] G. F. Kinney and K. J. Graham, *Explosive Shocks in Air*, 2nd ed. New York, NY, USA: Springer Science, 1985.

[2] Y. B. Zel'dovich and Y. P. Raizer, *Physics of Shock Waves and High-Temperature Hydrodynamic Phenomena.* New York, NY, USA: Academic Press, 1966.

[3] W. E. Baker, P. A. Cox, P. S. Westine, J. J. Kulesz, and R. A. Strehlow, *Explosion Hazards and Evaluation.* Amsterdam, Netherlands: Elsevier Science, 1983.

[4] C. E. Needham *Blast Waves*, 2nd ed. Berlin: Springer, 2010.

[5] F. P. Lees, *Loss Prevention in the Process Industries: Hazard Identification, Assessment and Control*, 2nd ed. Oxford, UK: Butterworth-Heinemann, 1996.

[6] E. Salzano, B. Picozzi, S. Vaccaro, and P. Ciambelli, "Hazard of pressurized tanks involved in fires," *Ind. Eng. Chem. Res.*, vol. 42, no. 8, pp. 1804–1812, 2003, http://dx.doi.org/10.1021/ie020606r.

[7] V. Molkov and S. Kashkarov, "Blast wave from a high-pressure gas tank rupture in a fire: Stand-alone and under-vehicle hydrogen tanks," *Int. J. Hydrogen Energy*, vol. 40, no. 36, pp. 12581–12603, 2015, http://dx.doi.org/10.1016/j.ijhydene.2015.07.001.

[8] R. Tschirschwitz et al., "Mobile gas cylinders in fire: Consequences in case of failure," *Fire Saf. J.*, vol. 91, pp. 989–996, 2017, http://dx.doi.org/10.1016/j.firesaf.2017.05.006.

[9] M. E. Beyer, "Blast loads behind vertical walls," in *Explosive Safety Seminar*, 1986.

[10] J. Wu, J. Liu, and Q. Yan, "Effect of shock wave on fabricated anti-blast wall and distribution law around the wall under near surface explosion," *Trans. Tianjin Univ.*, vol. 14, no. S1, pp. 514–518, 2008, http://dx.doi.org/10.1007/s12209-008-0088-5.

[11] W. Xiao, M. Andrae, and N. Gebbeken, "Experimental and numerical investigations on the shock wave attenuation performance of blast walls with a canopy on top," *Int. J. Impact Eng.*, vol. 131, pp. 123–139, Sep 2019, http://dx.doi.org/10.1016/j.ijimpeng.2019.05.009.

[12] L. Chen, R. Xu, Q. Fang, Y. Zheng, Z. Li, and M. Cao, "Response characteristics of gabion wall under large TNT-equivalent explosives," *J. Struct. Eng.*, vol. 148, no. 8, Aug 2022, http://dx.doi.org/10.1061/(ASCE)ST.1943-541X.0003413.

[13] X. Q. Zhou and H. Hao, "Prediction of airblast loads on structures behind a protective barrier," *Int. J. Impact Eng.*, vol. 35, no. 5, pp. 363–375, 2008, http://dx.doi.org/10.1016/j.ijimpeng.2007.03.003.

[14] J. Soukup, F. Klimenda, J. Skočilas, and M. Žmindák, "Finite element modelling of shock wave propagation over obstacles," *Manuf. Technol.*, vol. 19, no. 3, pp. 499–507, 2019, http://dx.doi.org/10.21062/ujep/319.2019/a/1213-2489/MT/19/3/499.

[15] A. K. Taha, Z. Gao, D. Huang, and M. S. Zahran, "Numerical investigation of a new structural configuration of a concrete barrier wall under the effect of blast loads," *Int. J. Adv. Struct. Eng.*, vol. 11, no. S1, pp. 19–34, 2019., http://dx.doi.org/10.1007/s40091-019-00252-8.

[16] Y. Skob, M. Ugryumov, and Y. Dreval, "Numerical modelling of gas explosion overpressure mitigation effects," *Mater. Sci. Forum*, vol. 1006, pp. 117–122, 2020., http://dx.doi.org/10.4028/www.scientific.net/MSF.1006.117.

[17] W. Attia, S. Elwan, and I. Kotb, "Investigating the effect of the geometry of RC barrier walls on the blast wave propagation," *Int. J. Saf. Secur. Eng.*, vol. 11, no. 3, pp. 255–268, 2021, http://dx.doi.org/10.18280/ijsse.110306.

[18] N. Gebbeken, P. Warnstedt, and L. Rüdiger, "Blast protection in urban areas using protective plants," *Int. J. Prot. Struct.*, vol. 9, no. 2, pp. 226–247, 2018, http://dx.doi.org/10.1177/2041419617746007.

[19] E. C. J. Gan, A. Remennikov, and D. Ritzel, "Investigation of trees as natural protective barriers using simulated blast environment," *Int. J. Impact Eng.*, vol. 158, pp. 104004, 2021, http://dx.doi.org/10.1016/j.ijimpeng.2021.104004.

[20] R. S. Browning, R. J. Dinan, and J. S. Davidson, "Blast Resistance of Fully Grouted Reinforced Concrete Masonry Veneer Walls," *J. Perform. Constr. Facil.*, vol. 28, no. 2, pp. 228–241, 2014, http://dx.doi.org/10.1061/(ASCE)CF.1943-5509.0000434.

[21] M. Jin, Y. Hao, and H. Hao, "Numerical study of fence type blast walls for blast load mitigation," *Int. J. Impact Eng.*, vol. 131, pp. 238–255, 2019, http://dx.doi.org/10.1016/j.ijimpeng.2019.05.007.

[22] T. L. S. Quaresma, T. D. Ferreira, and S. S. V. Vianna, "A hybrid BML-fractal approach for the mean reaction rate modelling of accidental gas explosions in partially confined obstructed geometries," *Process Saf. Environ. Prot.*, vol. 152, pp. 414–426, Aug 2021, http://dx.doi.org/10.1016/j.psep.2021.06.008.

[23] C. Y. Tham, "Numerical simulation on the interaction of blast waves with a series of aluminum cylinders at near-field," *Int. J. Impact Eng.*, vol. 36, no. 1, pp. 122–131, Jan 2009, http://dx.doi.org/10.1016/j.ijimpeng.2007.12.011.

[24] J. Trajkovski, R. Kunc, J. Perenda, and I. Prebil, "Minimum mesh design criteria for blast wave development and structural response - MMALE method," *Lat. Am. J. Solids Struct.*, vol. 11, no. 11, pp. 1999–2017, 2014, http://dx.doi.org/10.1590/S1679-78252014001100006.

[25] M. L. Costa No. and G. Doz, ""Estudo numérico das pressões de onda de choque em diferentes meios e sua transmissão," *Rev. Sul-americana Eng Estrutural*, vol. 14, no. 2, 2017, http://dx.doi.org/10.5335/rsaee.v14i2.7219.

[26] I. Cernak, "Animal models for concussion: Molecular and cognitive assessment - Relevance to sport and military concussions," in *Brain Neurotrauma*, F. H. Kobeissy, Ed., Gainsville, FL, USA: CRC Press, 2015, pp. 674–687.

[27] E. A. Rodriguez and W. Schofield, *Comparison of Blast Pressures and Effects Methodologies with Application to South Texas Units 3 & 4*. Washington, DC, USA: Energy Research Inc., 2009.

[28] A. Bolonkin, "Cumulative thermonuclear inertial reactor," *Energy Sustain. Soc.*, vol. 6, no. 1, pp. 8, 2016, http://dx.doi.org/10.1186/s13705-016-0074-z.

[29] Y. A. Çengel and M. A. Boles, *Thermodynamics: An Engineering Approach*, 8th ed. New York, NY, USA: McGraw-Hill, 2014.

[30] Associação Brasileira de Normas Técnicas, *Central de Gás Liquefeito de Petróleo – GLP*, NBR 13523, 2019.

[31] T. R. C. Moura, M. L. Costa No., and G. N. Doz, "Numerical analysis of the explosion of gas tanks using computational fluid dynamics," *Rev. IBRACON Estrut. Mater.*, vol. 16, no. 4, 2023, http://dx.doi.org/10.1590/s1983-41952023000400008.

[32] A. Borg, B. Paulsen Husted, and O. Njå, "The concept of validation of numerical models for consequence analysis," *Reliab. Eng. Syst. Saf.*, vol. 125, pp. 36–45, May 2014, http://dx.doi.org/10.1016/j.ress.2013.09.009.

[33] B. Luccioni, D. Ambrosini, and R. Danesi, "Blast load assessment using hydrocodes," *Eng. Struct.*, vol. 28, no. 12, pp. 1736–1744, Oct 2006, http://dx.doi.org/10.1016/j.engstruct.2006.02.016.

[34] D. G. Song, S. H. Jung, and E. S. Kim, "Structure integrity evaluation of gas protective wall for new construction method using strength test and numerical analysis," *J. Mech. Sci. Technol.*, vol. 35, no. 3, pp. 1143–1151, 2021, http://dx.doi.org/10.1007/s12206-021-0227-7.

[35] T. R. C. Moura, M. L. Costa No., and G. N. Doz, "Uso de muro de concreto como barreira física para mitigação dos efeitos de explosão de tanques de gás," in *Congresso Brasileiro do Concreto*, 2022.

[36] T. Lechat, A. Emmanuelli, D. Dragna, and S. Ollivier, "Propagation of spherical weak blast waves over rough periodic surfaces," *Shock Waves*, vol. 31, no. 4, pp. 379–398, Jun 2021, http://dx.doi.org/10.1007/s00193-021-01024-8.

Author contributions: TRCM: conceptualization, methodology, formal analysis, software, original draft writing; MLCN: guidance, supervision, formal review, software, correction, editing; GND: guidance, supervision, formal review, correction, editing.

Editors: Antonio Carlos dos Santos, Guilherme Aris Parsekian.